Tartrate-Resistant Acid Phosphatase Deficiency in the Predisposition to Systemic Lupus Erythematosus

DOI:
10.1002/art.39810

Document Version
Accepted author manuscript

Tartrate-Resistant Acid Phosphatase Deficiency in the Predisposition to Systemic Lupus Erythematosus

Journal:	*Arthritis & Rheumatology*
Manuscript ID	ar-15-1249.R1
Wiley - Manuscript type:	Full Length
Date Submitted by the Author:	14-Apr-2016
Complete List of Authors:	An, Jie; University of Washington, Department of Medicine Briggs, Tracy; University of Manchester, Genetic Medicine Dumax-vorzet, Audrey; University of Manchester, Genetic Medicine Alarcón-Riquelme, Marta E.; Centro de Genómica e Investigaciones Oncológicas (GENYO) Pfizer-Universidad de Granada-Junta de Andalucía, ; Oklahoma Medical Research Foundation, Arthritis and Clinical Immunology Program Belot, Alexandre; University of Lyon, Pediatric Rheumatology Unit Beresford, Michael; University of Liverpool, Institute of Child Health Bruce, Ian; The University of Manchester, Institute of Inflammation and Repair; Central Manchester University Hospitals NHS Foundation Trust, NIHR Manchester Musculoskeletal Biomedical Research Unit Carvalho, Claudia; Universidade do Porto, Lab Imunogenetics & Autoimmu and NeuroScien Chaperot, Laurence; Immunobiology & Immunotherapy of Cancers, INSERM U823/UJF/EFS Frostegard, Johan; Karolinska Institutet, Medicine Plumas, Joel; Immunobiology & Immunotherapy of Cancers, INSERM U823/UJF/EFS Rice, Gillian; Manchester Academic Health Science Centre, University of Manchester, Genetic Medicine Vyse, Tim; King's College London, Division of Genetics & Molecular Medicine; Guy's Hospital, Division of Immunology, Infection & Inflammatory Disease Wiedeman, Alice; University of Washington, Department of Medicine crow, yanick; University of Manchester, Genetic Medicine; Institut Imagine, Laboratory of Neurogenetics and Neuroinflammation Elkon, Keith B.; University of Washington, Head, Division of Rheumatology
Keywords:	Systemic lupus erythematosus (SLE), Interferon, Tartrate-Resistant Acid Phosphatase, Osteopontin, Spondyloenchondrodysplasia
<B>Disease Category: Please select the category from the list below that best describes the content of your manuscript.:	Systemic Lupus Erythematosus

Tartrate-Resistant Acid Phosphatase Deficiency in the Predisposition to Systemic Lupus Erythematosus

Jie An[*,#,2], Tracy A Briggs[*,#,2], Audrey Dumax-vorzet[2], Marta Alarcón Riquelme[3,4], Alexandre Belot[5], Michael Beresford[6], Ian Bruce[7], Claudia Carvalho[8], Laurence Chaperot[9], Johan Frostegård[10], Joel Plumas[9], Gillian I Rice[2], Tim J Vyse[11], Alice Wiedeman[1], Yanick J Crow[2,12], Keith B Elkon[#,1]

[1]Division of Rheumatology, Department of Medicine & Immunology, University of Washington, Seattle, WA98109, USA
[2]Manchester Academic Health Science Centre, University of Manchester, Genetic Medicine, Manchester, UK
[3]Centro de Genómica e Investigación Oncológica Pfizer-Universidad de Granada-Junta de Andalucía (GENYO), Granada, Spain
[4]Arthritis and Clinical Immunology Program, Oklahoma Medical Research Foundation, Oklahoma City, Oklahoma, USA
[5]Pediatric Rheumatology Unit, Femme Mère Enfant Hospital, Hospices Civils de Lyon, INSERM U1111, University of Lyon, France
[6]Department of Women's and Children's Heath, Institute of Translational Medicine, University of Liverpool, UK
[7]Arthritis Research UK Epidemiology Unit, Institute of Inflammation and Repair, The University of Manchester, and NIHR Manchester Musculoskeletal Biomedical Research Unit, Central Manchester University Hospitals NHS Foundation Trust, Manchester Academic Health Science Centre, Manchester, UK
[8]Lab Imunogenetics & Autoimmu and NeuroScien, Unidade Multidisciplinar Invest Biomed, Inst Ciencias Biomed Abel Salazar/ Universidade do Porto (C.C.), Porto, Portugal
[9]INSERM U823/UJF/EFS, Immunobiology & Immunotherapy of Cancers, La Tronche, France
[10]IMM, Unit of Immunology and Chronic Disease, Karolinska Institutet, Stockholm, Sweden
[11]King's College London, Division of Genetics & Molecular Medicine, Division of Immunology, Infection & Inflammatory Disease, Guy's Hospital, London, UK
[12]Institut Imagine, Laboratory of Neurogenetics and Neuroinflammation, 24 boulevard du Montparnasse, Paris, 75015, France

*These authors contributed equally to this work. [#]Corresponding authors

Abstract

Objectives: Mutations in *ACP5*, encoding tartrate-resistant acid phosphatase (TRAP), cause the immuno-osseous disorder Spondyloenchondrodysplasia, that includes systemic lupus erythematosus (SLE) and a type I interferon signature as disease features. Our aims were to identify TRAP substrates, determine the consequences of TRAP deficiency in immune cells, and assess whether *ACP5* mutations are enriched in sporadic SLE.

Methods: Interaction between TRAP and binding partners was tested by a yeast-2-hybrid screen, confocal microscopy and by immunoprecipitation/western blot analysis. TRAP knockdown was performed by siRNA and phosphorylation of osteopontin (OPN) by mass spectrometry. Nucleotide sequence analysis of *ACP5* was performed by Sanger or Next GEN sequencing.

Results: TRAP and OPN co-localized and interacted in human macrophages and plasmacytoid dendritic cells (pDCs). TRAP dephosphorylated three serine residues on specific OPN peptides. TRAP knockdown resulted in increased OPN phosphorylation and increased nuclear translocation of IRF7 and P65, with resultant heightened expression of interferon-stimulated genes, IL-6 and TNF following TLR9 stimulation. An excess of heterozygous *ACP5* missense variants was observed in SLE compared to controls (p=0.04) and transfection experiments revealed a significant reduction in TRAP activity in a number of variants.

Conclusions: Our findings indicate that TRAP and OPN co-localize and that OPN is a substrate for TRAP in human immune cells. TRAP deficiency in pDCs leads to increased interferon-alpha production, providing at least a partial explanation for how *ACP5* mutations cause lupus in the context of Spondyloenchondrodysplasia. Detection of *ACP5* missense variants in a lupus cohort suggests that impaired TRAP function may increase susceptibility to sporadic lupus.

Tartrate-resistant acid phosphatase (TRAP) is a member of the purple acid phosphatase family and is also referred to as type 5 acid phosphatase. It is predominantly expressed in cells of monocytic lineage, including osteoclasts, macrophages and dendritic cells (DCs) (1-3). There are two isoforms of the TRAP enzyme: TRAP5a and TRAP5b, with TRAP5b being produced by post-translational modification of TRAP5a. TRAP5b is the major isoform of TRAP secreted by osteoclasts, and TRAP5b activity has been shown to correlate with osteoclast number and activity in the serum, in both rat and human studies (4-6). In contrast, macrophages and DCs are believed to secrete TRAP5a as the predominant isoform, and TRAP5a is a nonspecific marker for macrophage activation (7, 8). Most studies of TRAP function relate to its role in the osteoclast, where extracellular TRAP has been strongly implicated in the regulation of osteoclast attachment and migration, particularly via the dephosphorylation of osteoclast-secreted osteopontin (OPN) (9). OPN is a highly phosphorylated, multifunctional glycoprotein that is secreted into biological fluids by many cell types including osteoclasts, macrophages and T cells (10). OPN is known to be a key protein in bone mineralization, and it is thought that phosphorylated OPN facilitates attachment of the osteoclast to the resorbing bone matrix. Consequently, OPN dephosphorylated by secreted TRAP leads to osteoclast release and migration (9).

Previously, we and others reported that biallelic mutations in gene *ACP5*, which encodes TRAP, result in a rare pediatric disorder named Spondyloenchondrodysplasia (SPENCD) (11, 12). Patients with SPENCD demonstrate a skeletal dysplasia reminiscent of that observed in the *ACP5* knockout mouse (13). Interestingly, however, patients also manifest a variable neurological and autoimmune phenotype. These autoimmune features include ANA and anti-dsDNA autoantibodies, autoimmune thrombocytopenia purpura and systemic lupus erythematosus (SLE). Patients with SPENCD consistently demonstrate an overexpression of interferon (IFN)-stimulated genes (ISGs) in whole blood, an IFN signature, although the link from TRAP deficiency to IFN signaling remains unexplained.

Initial studies have implicated OPN as potentially relevant to the pathology of SPENCD (11, 12). OPN, also known as ‘Early T-cell Activation Factor’ (14), is reported to be involved in diverse immune processes such as macrophage activation, inflammation and leukocyte recruitment, many of which are phosphorylation-dependent. It also plays a critical role in the efficient development of Th1 immune responses in T cells. Of note, polymorphisms in *OPN* and increased serum OPN levels have been associated with elevated IFN-alpha (IFN-α) levels in individuals with SLE (15). In the mouse, OPN has been shown to be integral to IFN-α production in plasmacytoid dendritic cells (pDC) - a major source of type I IFN (16).

Studies to date have highlighted SPENCD as a rare Mendelian cause of lupus and suggest an association between TRAP, OPN and IFN metabolism. The aim of our research was to decipher the detailed cellular pathways linking these molecules, and to understand how a loss of TRAP activity predisposes to autoimmune disease, particularly SLE.

Materials and Methods

Confocal microscopy

A Gen 2.2 pDC line was stained for immunofluorescence microscopy following adherence on polylysine slides. M-CSF-derived human macrophages derived from CD14+ circulating precursors were stained for immunofluorescence analysis in 4-chamber slides on day 5 (plated at 500,000 cells/ml per chamber on Day 0). TRAP, OPN, IRF7 and NFkB were detected with anti-TRAP 5a rabbit sera (17), mouse monoclonal anti-OPN antibody (Novus Biologicus), Rabbit polyclonal anti-IRF7 and anti-P65 (Santa Cruz) respectively, followed by secondary FITC labeled donkey anti-rabbit IgG (TRAP, IRF7, P65) and AF-555 donkey anti-mouse (OPN). Nuclei were stained with DAPI. Stained cells were viewed with a Zeiss LSM 510 confocal microscope with a 1.4 NA 63 x oil immersion lens. The images were analyzed by ImageJ. Three focal planes were analyzed with ~20 cells in each focal plane derived from two independent experiments. Nuclear translocation was quantified as the intensity of the IRF7/NFkB signal within the DAPI-positive nucleus as a ratio to that in the cytoplasm.

RNA and cDNA preparation and quantitative real-time PCR

Total RNA was isolated from pDCs using the RNeasy mini kit (Qiagen, Valencia, CA). cDNA was synthesized using 100 ng RNA with the high-capacity cDNA RT-kit with random primers (Applied Biosystems, Foster City, CA). Reactions in duplicate were run on an ABI StepOne Plus using primers for 18S, ACP5, IFI27, CXCL10, IFI44L, PKR, and Mx1 (Supplementary Table 2). A two-stage cycle of 95°C for 15 s and 60°C for 1 min was repeated for 40 cycles followed by a dissociation stage. Threshold cycle values were set as a constant threshold at 0.2, and fold changes in gene expression were then calculated using the $2^{-\Delta\Delta CT}$ method.

Western blot

Cells were lysed in lysis buffer composed of 0.5% NP-40 in 1X TBST, and 20 µg protein from each sample was loaded onto SDS-PAGE for western blot. The dilution of anti-TRAP antibody was 1:1000 (USB, USA) and the dilution of anti-OPN was 1:1000 (R&D System, USA). Signals were detected with the ECL detection system and film (GE Healthcare, Piscataway, NJ, USA). Quantitation was carried out using BioRad imaging system (BioRad, USA) with normalization against the intensity of β-Actin. Quantitative infrared western blots were carried out with lysates of HEK293 cells that were transiently transfected with different homozygous *ACP5* variants, using primary mouse anti-HA (Sigma-Aldrich) and rabbit anti-tubulin (Sigma), with secondary IRDye 800CW goat anti-mouse (LICOR Biosciences) and IRDye 680RD goat anti-rabbit secondary IgG (LICOR Biosciences). HA tag antibody was used, rather than TRAP antibody to exclude potential interference of point mutations with epitope recognition. Quantitation of bands was performed using Odyssey analysis software (LICOR Biosciences).

Yeast-two-hybrid screen.

A yeast-two-hybrid screen was performed by Hybrigenics services (www.hybrigenics-services.com) using an N-LexA-ACP5-C fusion protein and an N-Gal4-ACP5-C fusion protein on a Human Macrophage cDNA library from

monocyte-derived macrophages from healthy donors. The N-Gal4-ACP5-C fusion yielded 36 positive clones, which were assessed for interactions and categorized as A to E according to predicted confidence in results, with A indicating the highest degree of confidence in the interaction.

Generation of pDC and THP1 TRAP knockdown cell lines

Gen 2.2 pDC line or THP1 cells were transfected by TRAP5 or non-target shRNA control MISSION® shRNA Lentiviral Transduction Particles (Sigma) following the manufacturer's instructions. The stable pDC lines or THP1 cell lines with TRAP5 specific shRNA or scrambled shRNA were established after puromycin selection. The knockdown of TRAP was confirmed by qPCR with ACP5-specific primers (Supplementary table 2).

Phosphorylation analysis by mass spectrometry

TRAP knockdown THP1 cells were differentiated into macrophage-like cells by PMA (20nM) stimulation O/N. Cells were lysed with 6M Urea in 50mM Ammonium Bicarbonate. Proteins from cell lysate or recombinant Osteopontin were reduced by TCEP for 1 hour at 37°C and alkylated with Iodoactamide for 1 hour at room temperature in the dark. Proteins were digested by Trypsin at 1:50 (Enzyme: Protein) ratio O/N at 37°C. The peptides were then washed three times and desalted by C18 columns. Phosphopeptides were enriched by TiO2 column and desalted by Graphite columns according to the manufacturer's instruction. Phosphopeptides from recombinant Osteopontin (R&D System, USA) were analyzed by UPLC (Waters, USA) coupled with LTQ-OrbiTrap mass spectrometer (Thermal Scientific, USA). Phosphopeptides from cell lysates were analyzed by UPLC (Waters, USA) coupled with OrbiTrap Fusion mass spectrometer (Thermal Scientific, USA).

Subjects

DNA samples were collected from patients with confirmed lupus as defined by ACR criteria (18) and from controls. A total of 592 control samples were obtained from 92 Swedish, 189 Portuguese, 61 British and 187 mixed European individuals. 975 lupus samples were obtained from 240 Swedish adults, 162 Portuguese adults, 129 pediatric and 352 adult British patients and 92 Argentinian adults. Appropriate consents and ethical approvals were in place in each research group from which samples were obtained.

Sequence analysis

Sanger sequencing was undertaken in 890 lupus patients and all controls. PCR amplification of all coding exons of *ACP5* was performed (sequences available on request). Purified PCR amplification products were sequenced using dye-terminator chemistry and electrophoresed on an ABI 3130 (Applied Biosystems) capillary sequencer. As genetic techniques evolved over time, targeted enrichment and sequencing was subsequently undertaken in 85 different individuals with pediatric SLE. Enrichment was undertaken using SureSelect Human All Exon kits following the manufacturer's protocol (Agilent Technologies), and samples were paired-end sequenced on an Illumina HiSeq 2000 platform. Sequence data were mapped using Burrows-Wheeler Aligner using the hg18 (NCBI36) human genome as a reference. Data from 200 selected candidate lupus genes, including for *ACP5*, was extracted. Variants

were called using the Short Oligonucleotide Analysis Package, with medium stringency. Variants were confirmed by Sanger sequencing.

Mutation description is based on the reference complementary DNA (cDNA) sequence NM_001111035, with the ATG initiation site situated at the beginning of exon 4 and the termination codon in exon 7. The pathogenicity of variants was analyzed using Alumut, SIFT, PolyPhen and in the context of the crystal structure (19). Minor allele frequency was assessed using the Exome Aggregation Consortium (ExAC) database (exac.broadinstitute.org/).

Transient constructs

Wild type human *ACP5* cDNA coupled to an in frame Strep or HA tag was cloned into pcDNA3.2/GW/V5/D-TOPO vector (Invitrogen) and site-directed mutagenesis was performed to introduce individual point mutations into the *ACP5*-HA followed by confirmatory Sanger sequencing. The pcDNA3.2/GW/V5/D-TOPO without any *ACP5* cDNA insert (empty vector) was used as a control. HEK293 cells were transfected O/N with 4 µg plasmid DNA using 10 µl Lipofectamine 2000 (ThermoFisher Scientific) according to the manufacturer's instructions. In preliminary studies, we verified that Monomeric and cleaved TRAP were both detected in cell lysates while only monomeric TRAP was detected in supernatant using an anti-TRAP antibody and western blot. In addition, glycosylation appeared similar between Wild type and mutant protein as determined by Endo-H and PNGase sensitivity (data not shown).

TRAP phosphatase activity

BioMol Green assay was undertaken by incubating 1 µg human recombinant TRAP and 1 µg human recombinant or bovine milk OPN together in 0.4M sodium acetate and 200mM sodium tartrate (pH5.6) buffer at 37°C O/N. The free phosphate released from OPN was measured as per manufacturer's instructions (Enzo Life Sciences). Phosphate standards (Serial dilution from 2nmol to 0.031nmol) were used for the standard curve to quantify the released free phosphate. P-nitrophenyl phosphate (PnPP) assay was undertaken as previously described (17, 20). pNP concentration was normalized using protein concentration in the cell lysate. TRAP immunocytochemistry was undertaken by addition of naphthol AS-Bl phosphoric acid, which hydrolysed to naphthol AS-BI in the presence of TRAP and coupled with fast garnet GBC forming insoluble maroon deposits at the site of activity.

Statistics

Statistical significance between groups was determined by unpaired/paired t test or Chi squared test where appropriate. Correlations between parameters were assessed using the Pearson correlation analysis and linear regression analysis. *p=<0.05 and **p=<0.01. Graphs and statistical analyses were performed using Prism software (v 4; GraphPad Software).

Results

TRAP colocalizes and physically interacts with OPN in pDCs and macrophages.

Since OPN is a substrate for TRAP in osteoclasts (21), we asked whether this was also the

case in macrophages and pDCs. As shown in Fig.1A, OPN and TRAP co-localized both in the unstimulated human pDC line Gen 2.2 (22) (hereafter referred to as pDC line) and human primary monocyte-derived macrophages as determined by confocal microscopy. We performed organelle studies and determined that both OPN and TRAP were localized in the Golgi apparatus (Suppl. Fig.1).

To examine whether OPN and TRAP interact physically, we performed a yeast-two-hybrid screen in a human macrophage cDNA library. Whilst there were no category A-C (high confidence) interacting partners of TRAP identified, six category D (moderate confidence) interacting partners were demonstrated, including OPN, a Golgi processing protein COG1, the transcription factor USF2 which is postulated to have a functional role in RANKL-dependent TRAP expression during osteoclast differentiation (23), and three genes of unknown name or function. To confirm OPN as an interacting partner, we over-expressed OPN and TRAP in HEK293 cells (Suppl. Fig.2) and performed immuno-blot analysis (Fig.1B). TRAP was co-precipitated when OPN was immunoprecipitated (Fig.1B, upper panel), whilst in the reciprocal experiment OPN was co-precipitated with TRAP (Fig.1B, lower panel). To verify that this interaction occurred in primary cells, we observed that when OPN was immunoprecipitated in monocyte-derived macrophages, TRAP was readily detected on the western blot (Fig.1C, upper panel). In the reciprocal experiment, OPN was co-precipitated with TRAP (Fig.1C, lower panel) Since the signal obtained with anti-OPN was much stronger than that precipitated by anti-TRAP (Fig.1C, lower panel), these results suggest that only some of the OPN is associated with TRAP. In summary, the yeast-two-hybrid and co-precipitation data, together with the confocal studies, indicate that OPN and TRAP interact with each other and that OPN is a substrate for TRAP in some human immune cells.

OPN is a substrate of TRAP *in vitro*.

OPN has the potential to be extensively modified by alteration of its phosphorylation state, as there are a number of serine/threonine phosphorylation sites distributed throughout the protein. The degree of phosphorylation varies depending upon the source of the OPN. For example, human and bovine milk OPN (bmOPN) contain 32 and 28 serine/threonine phosphorylation sites respectively. The degree of phosphorylation of other forms of OPN, such as recombinant OPN, is less certain (24, 25). To assess whether human OPN is a substrate for TRAP, human recombinant OPN (rOPN) was incubated with human recombinant TRAP (rTRAP) and the amount of free/liberated phosphate was measured by Biomol green assay. Phosphate release significantly increased when rOPN and rTRAP were incubated together, as was also seen in the combined bmOPN and rTRAP positive control, compared to other single buffer controls (Fig.2A). To determine the residues at which TRAP removed phosphates, we performed UPLC-LTQ-OrbiTrap mass spectrometry analysis of rOPN following incubation with rTRAP. Protein database search results revealed that TRAP consistently dephosphorylated two phospho-serine residues (Sp) in the peptide GKDSpYETSQLDDQSpAETHSHK and the first Sp in the peptide ISHELDSpASpSEVN (Fig.2B).

Knockdown of TRAP results in an increase in IFN-α, IL6 and TNF production

associated with increased nuclear translocation of IRF7 and NFkB.

Activation of TLR9 in pDCs leads to IRF7 and NFkB nuclear translocation resulting in the transcription of IFN-α**,** IL-6 and TNF (26). Since OPN was reported to associate with the TLR9-MyD88 signaling complex in pDCs in mice (16) and we have shown that TRAP can associate with OPN and dephosphorylate it, we investigated the effects of shRNA-mediated knockdown (KD) of TRAP in the pDC line. We established three pDC cell lines with stable KD of TRAP compared to empty vector and scramble shRNA controls in both unstimulated (average 67% KD) (Fig.3A) and stimulated pDC cells (average 75% KD) (Fig.3B). Consistent with a role for TRAP in the regulation of OPN function, a significant increase in IFN-α concentration was observed in the TRAP KD pDC lines compared to scrambled shRNA (control) following TLR9 stimulation with CpGA (Fig.3C). Consistent with the increase in IFN-α, the expression of the ISGs IFI27, CXCL10, IFI44L, PKR and Mx1, (Fig.3D) were increased in the TRAP KD pDC line. Of interest, stimulation of the TRAP KD pDC line with CpGB also lead to increased production of the cytokines TNF (Fig.3E) and IL6 (Fig. 3F).

To gain further insight into the mechanisms responsible for increased cytokine production, we examined the nuclear localization of the transcription factors IRF7 and NFkB, which are downstream of TLR9 in pDC. Whereas there was no difference in the localization of IRF7 and NFkB in unstimulated cells (Suppl. Fig.3), we observed significantly more IRF7 (Fig.4A) and NFkB (Fig.4B) nuclear translocation in the TRAP KD pDC line, compared to the control pDC line, following CpG stimulation. These data demonstrate that TRAP plays a role in the regulation of IFN-α**,** IL6 and TNF cytokine production in human pDCs. Consistent with the *in vitro* data, a number of SPENCD patients showed significant elevation of IL-6 (but not TNF) expression in whole blood (Suppl. Fig.4), in addition to the elevated IFN-α data already reported (11).

OPN is hyperphosphorylated in TRAP KD compared to control THP1 cells.

To further verify that TRAP regulates OPN function in pDCs, we determined whether there was differential phosphorylation of OPN in TRAP KD versus control pDC line. Due to the low expression level of OPN in the pDC line, attempts to detect phosphopeptides following CpG stimulation were unsuccessful. We therefore examined a TRAP KD THP1 cell line. Following PMA stimulation and differentiation to macrophage-like cells, TRAP KD THP1 cells consistently demonstrated an increased amount of hyperphosphorylated OPN quantified by LC-MS/MS, as compared to controls (Fig.5A). The hyperphosphorylated sites were within the same two peptides identified with rOPN (Fig.2B), and two of three of the phosphorylated sites were the same (Fig.5B and 5C). Hyperphosphorylation of OPN in TRAP KD cells further indicated that OPN is a substrate for TRAP in human immune cells and that TRAP regulation of OPN, by dephosphorylation, may regulate interferon production, as depicted in Fig.5D.

***ACP5* heterozygous variants in SLE.**

In view of the high prevalence of lupus in SPENCD (27) (11), we sought to determine whether TRAP influenced susceptibility to idiopathic SLE. To address this question, we sequenced all coding exons of the *ACP5* gene in 890 SLE patients and 529 healthy matched

controls by the Sanger method, and by NextGEN sequencing of a further 85 pediatric SLE patients. Patients and control populations were matched in terms of ethnicity for all samples except for 92 samples from Argentinian lupus patients and 187 mixed European control samples. An analysis of Hardy-Weinberg equilibrium and the frequency of three commonly occurring SNPs suggested that all groups were directly comparable. We assessed for rare, non-synonymous variants or canonical intronic variants within the cohorts as these were considered more likely to be of functional effect. We defined rare as a minor allele frequency (MAF) <0.002 in the ExAC database, which includes data for *ACP5* on approximately 120,000 control population alleles. A MAF of <0.002 was chosen as this is the MAF of the commonest disease causing variant observed in the mendelian interferonopathy Acardi-Goutieres syndrome (P193A mutation in *ADAR1* (28). This variant has unequivocal pathogenicity and we therefore considered that variants of up to this MAF may be disease causing. We observed an increased number of rare heterozygous missense *ACP5* variants in the SLE patients (15/975) compared to controls (2/529) (p=0.044). There was a total of 13 different rare variants in a total of 12 adults and 3 children and they were distributed across the assessed ethnic groups (5 British, 4 Swedish, 4 Portuguese and 2 Argentinian). When *in silico* testing was performed, the missense residues were moderately to well conserved in mammalian species, and the majority were predicted to destabilize the protein on *in silico* modeling (Supp. Table 1). One of the variants, Met264Lys, has previously been reported in the homozygous state in a patient with SPENCD (11).

To test whether the *ACP5* heterozygous variants identified in the SLE cohort could cause a reduction in TRAP activity, we produced HEK293 cells expressing homozygous *ACP5* constructs and subsequently co-transfections of wild type and variant constructs. In the lysate and supernatant of cells transiently transfected with eleven different homozygous variant constructs, a significant reduction of TRAP activity (assessed using PnPP assay) was observed in seven of the eleven variants compared to wild type (Fig.6A). This correlated well with cytochemical staining of transiently transfected homozygous HEK293 cells (Fig.6B). Quantitative western blot demonstrated that protein levels were minimally altered in the lysate (Fig.6C upper panel) and a Pearson's correlation coefficient of TRAP expression to activity (Supp. Fig.5) was low (R^2=0.1). This suggests that only around 10% of the variation in activity in the lysate could be attributed to variation in expression level. We therefore hypothesize that the origin of the majority of the variation in activity is not an absence of protein, but is due to an effect on catalytic activity. In contrast, in the supernatant, quantitative western blot demonstrated a reduction in protein levels in those variants in which activity levels were significant reduced (Fig.6C lower panel). The high Pearson's correlation coefficient between relative TRAP expression and activity (R^2=0.98) (Supp. Fig.5), suggests that over 97% of variation in activity can be attributed to variation in protein expression level. As quality control in secretory pathways is highly efficient at sifting misfolded protein to ensure that only correctly folded active proteins are secreted, we propose that some variants may be misfolded and degraded, thus reducing secretion into the supernatant.

We co-transfected WT and mutant constructs for five of the SLE variants to more accurately simulate the heterozygous situation in SLE patients. We chose to express four variants that demonstrated significantly reduced activity in the homozygous state, in addition to the Thr5Met variant for which *in silico* prediction was not possible since it lies outside of

the reported crystal structure. Four of the SLE variants showed a reduction in TRAP activity, which was statistically significant in the lysate of two and the supernatant of three *ACP5* variant constructs (Fig.6D). Whilst the activity of WT and mutant 1:1 co-transfections were reduced compared to WT and WT, this reduction was not beyond that seen with WT and empty vector suggesting that this was not a dominant negative effect. Western blot analysis was not possible in these cells due to the co-expression of WT and variant TRAP. However, equal expression of both constructs (WT and mutant/WT/empty vector) was confirmed by qPCR. Of note, since shRNA knockdown of TRAP to ~33% expression was sufficient to cause ISG upregulation following pDC stimulation (Fig.3D), we hypothesize that a number of these rare heterozygous *ACP5* missense variants are functionally and clinically relevant for lupus disease development due to reduced TRAP activity. Further assessments of sub-cellular localization and post-translational processing may identify further functional consequences of point mutations, especially those that do not appear to affect protein activity.

Discussion

In this study we investigated the role of TRAP and OPN in innate immunity in humans with special relevance to SPENCD and the systemic autoimmune disease SLE. We found that TRAP co-localized and physically interacted with OPN in pDCs and in macrophages, and that OPN is a substrate for TRAP. When TRAP expression was reduced in pDCs we observed that TLR9 stimulation caused an increased nuclear translocation of IRF7 and NFkB with associated elevation in IFN-α, ISGs, IL-6 and TNF expression - thus offering an explanation for the IFN signature and inflammatory phenotype in SPENCD patients. Our findings may be of relevance not only to the pathogenesis of SPENCD, but also to lupus susceptibility as, in a survey of SLE patients, we demonstrated an over-representation of heterozygous *ACP5* missense variants, several of which display impaired catalytic activity.

To understand the relationship between TRAP deficiency and type I IFN production in SPENCD patients, the hypothesis that we explored in this study stems from the work of Shinohara *et al*. (16) who reported that the association of OPN with the TLR9-MyD88 signaling complex was essential for IFN-α production in murine pDCs (16). However, in those studies, phosphorylation of OPN was not assessed. Activation of the TLR9-MyD88 signaling pathway within pDCs has been shown to lead to both IRF7 and NFkB nuclear translocation resulting in the transcription of IFN-α, IL-6 and TNF (26). We established further evidence for a role of TRAP in the regulation of this pathway. Specifically, when we knocked down TRAP expression in a pDC line, we observed that TLR9 stimulation caused increased nuclear translocation of both IRF7 and NFkB along with an elevation in IFN-α, IL6 and TNF, compared to control cell lines. These data are consistent with the clinical observation of significant elevation of IFN-α in SPENCD cases (11) and elevated IL-6 levels detected in several patients.

We propose that the increased IFN-α production following CpGA stimulation in TRAP deficient pDCs is secondary to the action of the persistent, unregulated action of the TLR9-MyD88-OPN signalosome, as illustrated in Fig.5D. Thus, TRAP deficiency would cause a lack of OPN dephosphorylation and deactivation, resulting in persistent formation of the OPN-TLR9-MyD88 complex, with increased IFN-α production and a predisposition to autoimmune disease. Unfortunately, we could not definitively confirm this possibility

experimentally as we were unable to assess OPN phosphorylation in pDC by LC-MS/MS (due to limited substrate availability from even 50 million cells in our pDC KD line). It therefore remains to be formally determined whether OPN is a physical component of the TLR9-MyD88 complex in human immune cells, or whether TRAP acts on a different, or even multiple, substrate(s) in this pathway.

The function of TRAP has previously been explored in another myeloid derived cell, the osteoclast. Ultrastructural immunohistochemistry revealed that, similar to OPN, TRAP is localized to the resorption lacuna, where it may directly contact bone OPN in an acidic environment (29). Here, TRAP dephosphorylation of OPN facilitated osteoclast migration during bone resorption (9). In TRAP deficient mice, delayed clearance of the microbial pathogen *Staphylococcus Aureus*, and a reduced population of macrophages in the peritoneal exudates was observed - suggesting that TRAP may directly or indirectly influence recruitment of macrophage to sites of microbial invasion (30). Concurrently, *in vitro* studies showed that phosphorylation-dependent interaction of OPN with its receptor regulated macrophage migration and activation (31). Whether or not TRAP regulation of OPN influences macrophage recruitment in SPENCD is yet to be determined.

It will be interesting to assess in further studies whether other potential TRAP substrates, including the additional possible interacting partners identified by the yeast-2-hybrid (if validated), may also be involved in the SPENCD phenotype, particularly relating to observed increased IL6 and TNF levels.

Loss of TRAP activity causes SPENCD, and nearly half of all SPENCD patients fulfilled ACR diagnostic criteria for SLE, whilst nearly all had positive anti-dsDNA and/or ANA antibody titers (11, 12). These findings suggest that TRAP might influence susceptibility to idiopathic SLE. Sequencing of the *ACP5* gene in nearly 1000 SLE patients demonstrated a significant excess of heterozygous *ACP5* missense variants in SLE patients compared to controls. In addition, using an *in vitro* transfection assay, we observed a reduction of TRAP activity with a number of the variants seen in SLE patients, indicating that impaired function of TRAP may play a role in the susceptibility to idiopathic lupus in a proportion of patients. The possibility that heterozygote *ACP5* variants may have pathogenic consequences is supported by the skeletal phenotype observed in the heterozygous *ACP5* knock-out mouse(13) , and we also note a cellular phenotype was observed with a lentiviral TRAP knockdown of 67%.

In conclusion, our findings indicate that TRAP and OPN co-localize, and that OPN is a substrate for TRAP in immune cells. Significantly, TRAP deficiency in pDCs leads to increased IFN-α production, providing at least a partial explanation for how biallelic *ACP5* mutations cause SLE in the context of SPENCD. Detection of heterozygous *ACP5* missense variants in lupus patients suggests that impaired function of TRAP may play a role in the susceptibility to idiopathic lupus.

Acknowledgements

We thank Dr Goran Andersson for kindly providing the TRAP antibody for confocal microscopy and Dr. Priska von Haller and Jimmy Eng for mass spectrometer technical and bioinformatics support. Dr Simon Lovell for performing *in silico* assessments of the SLE genetic variants and Drs. Xizhang Sun and Nalini Agrawal for technical support. We would

also like to thank the Exome Aggregation Consortium (ExAC), Cambridge, MA (URL: http://exac.broadinstitute.org) [03/2015]. TAB acknowledges funding from the National Institute for Health Research (NIHR), a L'Oréal-UNESCO UK & Ireland Fellowship for Women in Science and the NIHR Manchester Musculoskeletal Biomedical Research Unit. INB is an NIHR Senior Investigator and is funded by Arthritis Research UK, the NIHR Manchester Biomedical Research Unit and the NIHR/Wellcome Trust Manchester Clinical Research Facility. The views expressed in this publication are those of the author(s) and not necessarily those of the NHS, the National Institute for Health Research or the Department of Health. JA and AD acknowledge funding from The Alliance for Lupus Research. Y.J.C. acknowledges the European Research Council (GA 309449: Fellowship), and a state subsidy managed by the National Research Agency (France) under the "Investments for the Future" program bearing the reference ANR-10-IAHU-01.

References

1. Minkin C. Bone acid phosphatase: tartrate-resistant acid phosphatase as a marker of osteoclast function. Calcif Tissue Int. 1982;34:285-90.
2. Hayman AR, Macary P, Lehner PJ, Cox TM. Tartrate-resistant acid phosphatase (Acp 5): identification in diverse human tissues and dendritic cells. J Histochem Cytochem. 2001;49:675-84.
3. Hayman AR, Bune AJ, Bradley JR, Rashbass J, Cox TM. Osteoclastic tartrate-resistant acid phosphatase (Acp 5): its localization to dendritic cells and diverse murine tissues. J Histochem Cytochem. 2000;48:219-28.
4. Chu P, Chao TY, Lin YF, Janckila AJ, Yam LT. Correlation between histomorphometric parameters of bone resorption and serum type 5b tartrate-resistant acid phosphatase in uremic patients on maintenance hemodialysis. Am J Kidney Dis. 2003;41:1052-9.
5. Henriksen K, Tanko LB, Qvist P, Delmas PD, Christiansen C, Karsdal MA. Assessment of osteoclast number and function: application in the development of new and improved treatment modalities for bone diseases. Osteoporos Int. 2007;18:681-5.
6. Rissanen JP, Suominen MI, Peng Z, Halleen JM. Secreted tartrate-resistant acid phosphatase 5b is a Marker of osteoclast number in human osteoclast cultures and the rat ovariectomy model. Calcif Tissue Int. 2008;82:108-15.
7. Janckila AJ, Yam LT. Biology and clinical significance of tartrate-resistant acid phosphatases: new perspectives on an old enzyme. Calcif Tissue Int. 2009;85:465-83.
8. Hayman AR. Tartrate-resistant acid phosphatase (TRAP) and the osteoclast/immune cell dichotomy. Autoimmunity. 2008;41:218-23.
9. Ek-Rylander B, Flores M, Wendel M, Heinegard D, Andersson G. Dephosphorylation of osteopontin and bone sialoprotein by osteoclastic tartrate-resistant acid phosphatase. Modulation of osteoclast adhesion in vitro. J Biol Chem. 1994;269:14853-6.
10. Inoue M, Shinohara ML. Intracellular osteopontin (iOPN) and immunity. Immunol Res. 2011;49:160-72.
11. Briggs TA, Rice GI, Daly S, Urquhart J, Gornall H, Bader-Meunier B, et al. Tartrate-resistant acid phosphatase deficiency causes a bone dysplasia with autoimmunity and

a type I interferon expression signature. Nat Genet. 2011;43:127-31.
12. Lausch E, Janecke A, Bros M, Trojandt S, Alanay Y, De Laet C, et al. Genetic deficiency of tartrate-resistant acid phosphatase associated with skeletal dysplasia, cerebral calcifications and autoimmunity. Nat Genet. 2011;43:132-7.
13. Hayman AR, Jones SJ, Boyde A, Foster D, Colledge WH, Carlton MB, et al. Mice lacking tartrate-resistant acid phosphatase (Acp 5) have disrupted endochondral ossification and mild osteopetrosis. Development. 1996;122:3151-62.
14. Patarca R, Saavedra RA, Cantor H. Molecular and cellular basis of genetic resistance to bacterial infection: the role of the early T-lymphocyte activation-1/osteopontin gene. Crit Rev Immunol. 1993;13:225-46.
15. Trivedi T, Franek BS, Green SL, Kariuki SN, Kumabe M, Mikolaitis RA, et al. Osteopontin alleles are associated with clinical characteristics in systemic lupus erythematosus. J Biomed Biotechnol. 2011;2011:802581.
16. Shinohara ML, Lu L, Bu J, Werneck MB, Kobayashi KS, Glimcher LH, et al. Osteopontin expression is essential for interferon-alpha production by plasmacytoid dendritic cells. Nat Immunol. 2006;7:498-506.
17. Lang P, Andersson G. Differential expression of monomeric and proteolytically processed forms of tartrate-resistant acid phosphatase in rat tissues. Cell Mol Life Sci. 2005;62:905-18.
18. Tan EM, Cohen AS, Fries JF, Masi AT, McShane DJ, Rothfield NF, et al. The 1982 revised criteria for the classification of systemic lupus erythematosus. Arthritis Rheum. 1982;25:1271-7.
19. Strater N, Jasper B, Scholte M, Krebs B, Duff AP, Langley DB, et al. Crystal structures of recombinant human purple Acid phosphatase with and without an inhibitory conformation of the repression loop. J Mol Biol. 2005;351:233-46.
20. Ljusberg J, Ek-Rylander B, Andersson G. Tartrate-resistant purple acid phosphatase is synthesized as a latent proenzyme and activated by cysteine proteinases. Biochem J. 1999;343 Pt 1:63-9.
21. Andersson G, Ek-Rylander B, Hollberg K, Ljusberg-Sjolander J, Lang P, Norgard M, et al. TRACP as an osteopontin phosphatase. J Bone Miner Res. 2003;18:1912-5.
22. Chaperot L, Bendriss N, Manches O, Gressin R, Maynadie M, Trimoreau F, et al. Identification of a leukemic counterpart of the plasmacytoid dendritic cells. Blood. 2001;97:3210-7.
23. Liu Y, Shi Z, Silveira A, Liu J, Sawadogo M, Yang H, et al. Involvement of upstream stimulatory factors 1 and 2 in RANKL-induced transcription of tartrate-resistant acid phosphatase gene during osteoclast differentiation. J Biol Chem. 2003;278:20603-11.
24. Christensen B, Klaning E, Nielsen MS, Andersen MH, Sorensen ES. C-terminal modification of osteopontin inhibits interaction with the alphaVbeta3-integrin. J Biol Chem. 2012;287:3788-97.
25. Wang KX, Denhardt DT. Osteopontin: role in immune regulation and stress responses. Cytokine Growth Factor Rev. 2008;19:333-45.
26. Gilliet M, Cao W, Liu YJ. Plasmacytoid dendritic cells: sensing nucleic acids in viral infection and autoimmune diseases. Nat Rev Immunol. 2008;8:594-606.
27. Briggs TA, Rice GI, Adib N, Ades L, Barete S, Baskar K, et al.

Spondyloenchondrodysplasia Due to Mutations in ACP5: A Comprehensive Survey. J Clin Immunol. 2016;36:220-34.
28. Rice GI, Kasher PR, Forte GM, Mannion NM, Greenwood SM, Szynkiewicz M, et al. Mutations in ADAR1 cause Aicardi-Goutieres syndrome associated with a type I interferon signature. Nat Genet. 2012;44:1243-8.
29. Flores ME, Norgard M, Heinegard D, Reinholt FP, Andersson G. RGD-directed attachment of isolated rat osteoclasts to osteopontin, bone sialoprotein, and fibronectin. Exp Cell Res. 1992;201:526-30.
30. Bune AJ, Hayman AR, Evans MJ, Cox TM. Mice lacking tartrate-resistant acid phosphatase (Acp 5) have disordered macrophage inflammatory responses and reduced clearance of the pathogen, Staphylococcus aureus. Immunology. 2001;102:103-13.
31. Weber GF, Zawaideh S, Hikita S, Kumar VA, Cantor H, Ashkar S. Phosphorylation-dependent interaction of osteopontin with its receptors regulates macrophage migration and activation. J Leukoc Biol. 2002;72:752-61.
32. Ek-Rylander B, Andersson G. Osteoclast migration on phosphorylated osteopontin is regulated by endogenous tartrate-resistant acid phosphatase. Exp Cell Res. 2010;316:443-51.

Figure legends

Fig.1. Colocalization and interaction of TRAP and OPN in pDCs and primary human macrophages.
A, Confocal microscopy of TRAP (green) and OPN (red) with the overlay demonstrating partial colocalization in a pDC line Gen 2.2 (upper) and macrophages (lower). Representative image of four independent experiments. **B,** HEK293 cells were co-transfected with OPN and TRAP. After 48 hours, cells were lysed and target proteins immunoprecipitated (IP) with the antibodies as shown. Samples were resolved by SDS-PAGE and then immunoblotting (IB) performed with antibodies targeted to the antigens shown. Upper panel: anti-OPN IP followed by anti-TRAP IB; lower panel: anti-TRAP IP followed by anti-OPN IB. **C,** IP and immunoblotting were performed as in B, except that the lysates were made from primary macrophages stimulated with CpG-B for 18hours. Upper panel: anti-OPN IP followed by anti-TRAP IB; lower panel: anti-TRAP IP followed by anti-OPN. Key: The positive control was loaded in the first lane of each gel and IgG is the appropriate isotype control for each IP. Data derived from two independent experiments (B & C).

Fig.2. OPN is a substrate for TRAP.
A, Bovine milk OPN (bmOPN, 1µg) or rOPN (1µg) were incubated with rTRAP (1µg) overnight(32). Free phosphates were quantified by BioMol green assay with phosphate as standards; bmOPN, rOPN, rTRAP or reaction buffer only were used for negative control for background signal. *p=<0.05. **B,** Human rOPN (500 ng) was incubated with rTRAP (500 ng) overnight. The reaction mixtures were trypsin digested and subjected to LC-MS/MS for the detection of phosphorylated peptides from OPN protein. The three phosphorylation sites (Sp: phoshorylated Serine) on two peptides of OPN which were found to be dephosphorylated by TRAP are depicted in red. The reaction was performed in duplicate (A-C).

Fig. 3. Knockdown of TRAP increases production of IFN-α, ISGs, TNF and IL6 in pDCs.
Empty Vector, Scrambled shRNA or TRAP shRNA (3 different clones) transfected Gen 2.2 pDCs were either unstimulated (panel A), stimulated with CpG-A (panels B-D) or CpG-B (panel E and F) for 16 hours. **A and B**, ACP5 mRNA expression was measured by q-PCR and normalized to housekeeping gene 18s mRNA expression. **C,** IFN-α cytokine production was quantified by ELISA. **D**, IFN-stimulated genes IFI27, CXCL10, IFI44L, PKR and MX1 mRNA expression was measured by q-PCR and normalized to housekeeping gene 18s mRNA

expression. **E and F**, TNF and IL6 cytokine production was quantified by ELISA. *p=<0.05 and **p=<0.01. Data was derived from 6 independent experiments.

Fig.4: TRAP knockdown in pDCs increases nuclear translocation of IRF7 and NFkB. **A,** The pDC line, Gen 2.2, was stimulated with CpG-A for 1 hour and analyzed by confocal microscopy using DAPI (pseudo-green) to stain the nucleus and an antibody to the transcription factor, IRF7 (pseudo-red). A representative image is shown on the left and relative intensity of IRF7 nuclear translocation post stimulation was quantified in TRAP KD pDCs compared to scrambled shRNA control, as shown on the right. **B,** Confocal microscopy of DAPI and NFkB (p65 subunit) in a representative image from the pDC line Gen 2.2 stimulated with CpG-B for 1 hour is shown on the left, with quantification of relative intensity for NFkB nuclear translocation in TRAP KD pDCs compared to scrambled shRNA control presented on the right. The relative intensity of IRF7 and NFkB nuclear translocation post stimulation were quantified by ImageJ software and are shown in both cases in the graph. The experiments A and B were performed twice independently.

Fig.5. OPN is hyperphosphorylated in TRAP knockdown THP1 cells.
THP1 cells were transfected with scrambled shRNA or TRAP shRNA and PMA differentiated to macrophage-like cells. Phosphopeptides were prepared for mass spectrometry (LC-MS/MS) (see methods). Acquired OPN phosphopeptide counts were normalized to total peptides counts in the same mass spec run for the OPN phosphopeptides quantification between scrambled shRNA and TRAP shRNA samples. **A,** The abundance of phosphorylated OPN peptides in the TRAP shRNA compared to scrambled shRNA. **B,** The three specific serine residues in two peptides of OPN which were hyperphosphorylated in the TRAP shRNA are depicted in red. The data is derived from four independent experiments. C. A representative image for the mass spectrum of the phosphopeptide: ISHELDSASpSEVN. X axis indicated the mass to charge ratio (m/z) of the fragmented ions from the peptides and Y axis indicated the relative intensity of signal from each fragmented ion. **D**, Model for TRAP/OPN axis in the regulation of IFN-α. Step 1 illustrates phosphorylation, and thus activation, of iOPN (intracellular OPN), perhaps by a DNA ligand. Activated iOPN then forms a complex with TLR9 and MyD88 and, via IRF7, induces IFN-α production. Regulation of the pathway, as illustrated in the upper panel of Step 2, is achieved by dephosphorylation of OPN by TRAP, with subsequent inhibition of IFN-α induction. The lower panel in Step 2, demonstrates continued formation of the iOPN/MyD88/TLR signalosome with prolonged IFN-α production, due to a TRAP deficiency, as in SPENCD and possibly, some SLE cases.

Fig.6: TRAP activity in HEK293 cells transiently transfected with homozygous or heterozygous *ACP5* variants identified in a lupus cohort. A, PnPP activity measured in the cell lysate and supernatant of eleven homozygote variant constructs was compared to WT and empty vector (EV). TRAP activity was normalized to lysate protein concentration. **B,** TRAP activity was measured by immunocytochemistry, with purple staining intensity indicating activity level. EV (A) and WT (B) were compared to Thr5Met (C), Arg46Trp (D), Phe141Val (E), Thr183Lys (F), Val208Met (G), Glu213Gln (H), Met264Lys (I), Arg269Trp (J),

Arg272His (K) and His282Arg (L). **C,** Concurrent to PnPP assay (A) 10 µg of cell lysate and an equal volume of supernatant were analysed by quantitative western blot. Tubulin was used as loading control in cell lysates and quality control; its absence in supernatants indicates that supernatant proteins were secreted by intact cells. **D,** PnPP activity in the cell lysate and supernatant in five heterozygote variants was compared to WT and EV. Equal amounts of Strep-tagged WT and HA-tagged mutant *ACP5* were transfected. Expression of both constructs was confirmed by qPCR (data not shown). Mean values of 4 to 6 independent experiments are shown for A and D, representative images are shown from 4 independent experiments for B and C.

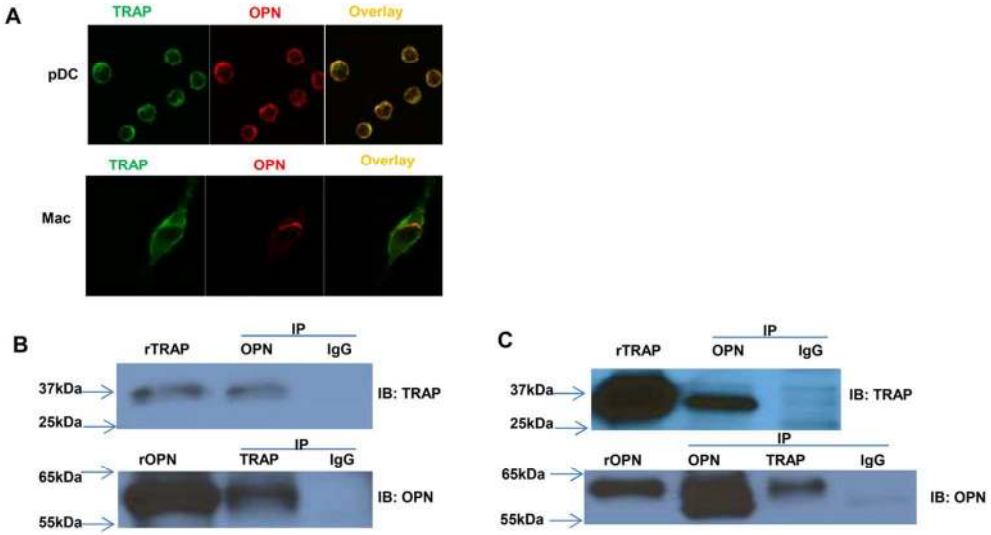

Figure1
115x70mm (300 x 300 DPI)

A

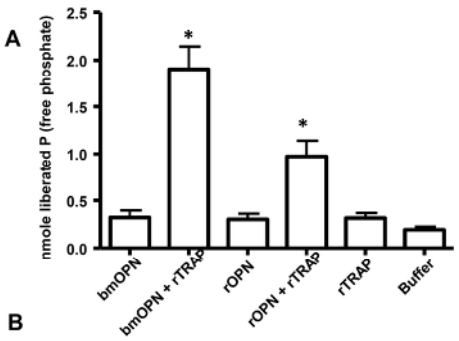

B

Sample No.	Protein probability	Protein Description	Peptide sequence
rOPN Only	1	Osteopontin	GKDSpYETSQLDDQSpAETHSHK
rOPN Only	1	Osteopontin	ISHELDSpASpSEVN
rOPN + rTRAP	1	Osteopontin	GKDSYETSQLDDQSAETHSHK
rOPN + rTRAP	1	Osteopontin	ISHELDSASpSEVN

Figure2
104x57mm (300 x 300 DPI)

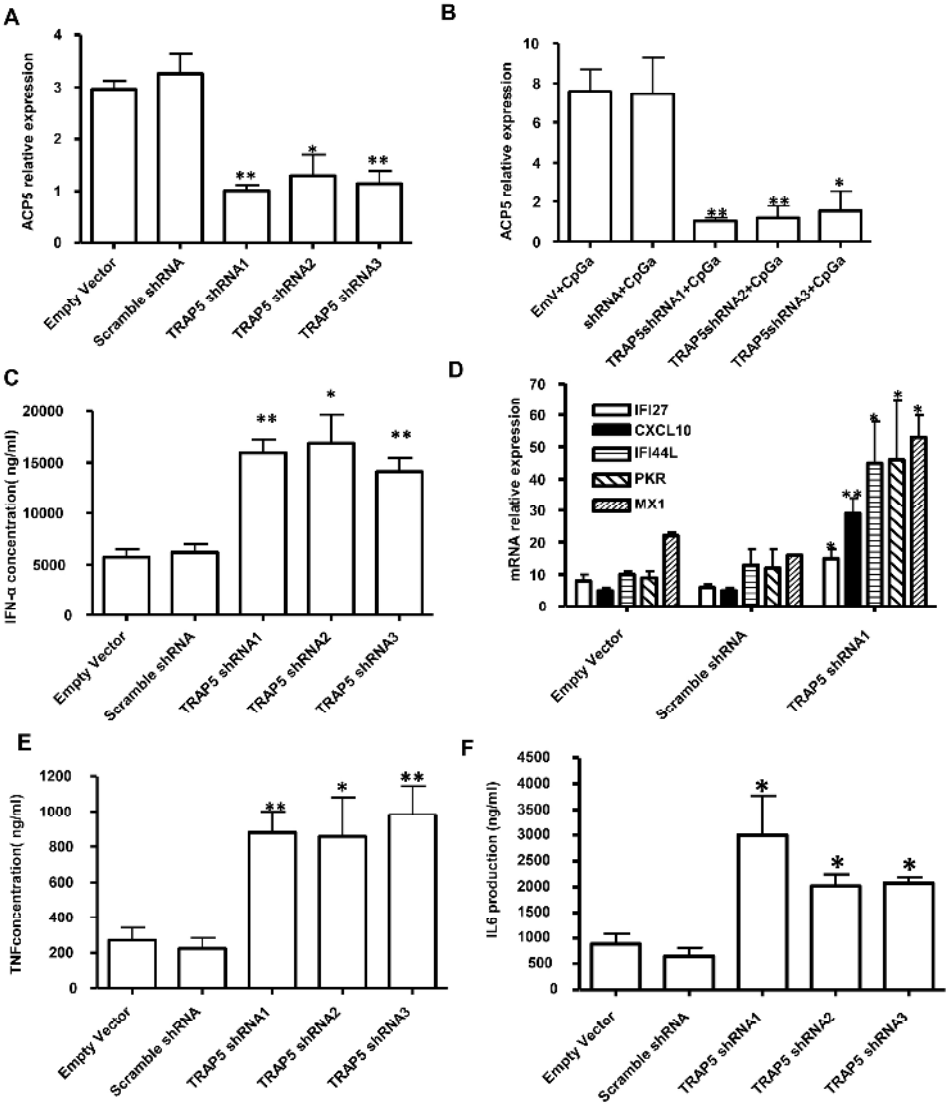

Figure3
215x243mm (300 x 300 DPI)

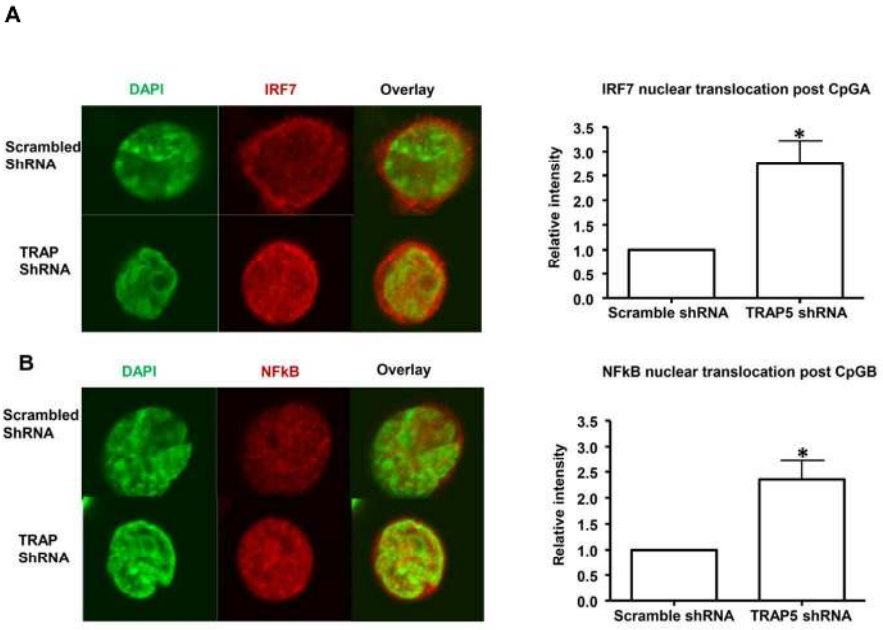

Figure4
130x90mm (300 x 300 DPI)

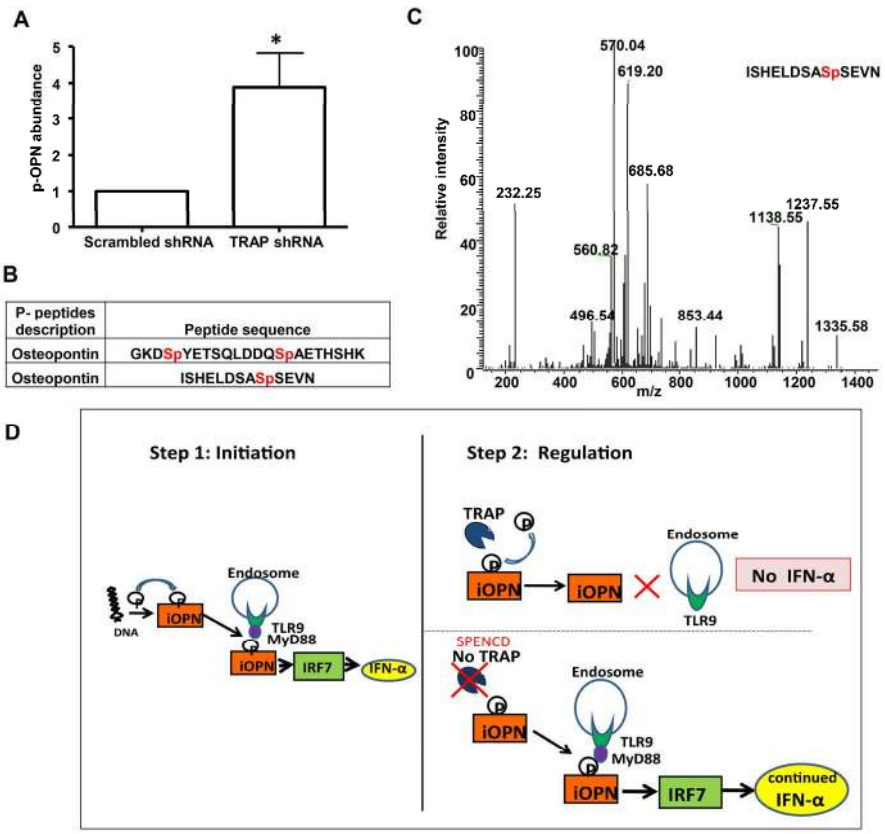

Figure5
163x140mm (300 x 300 DPI)

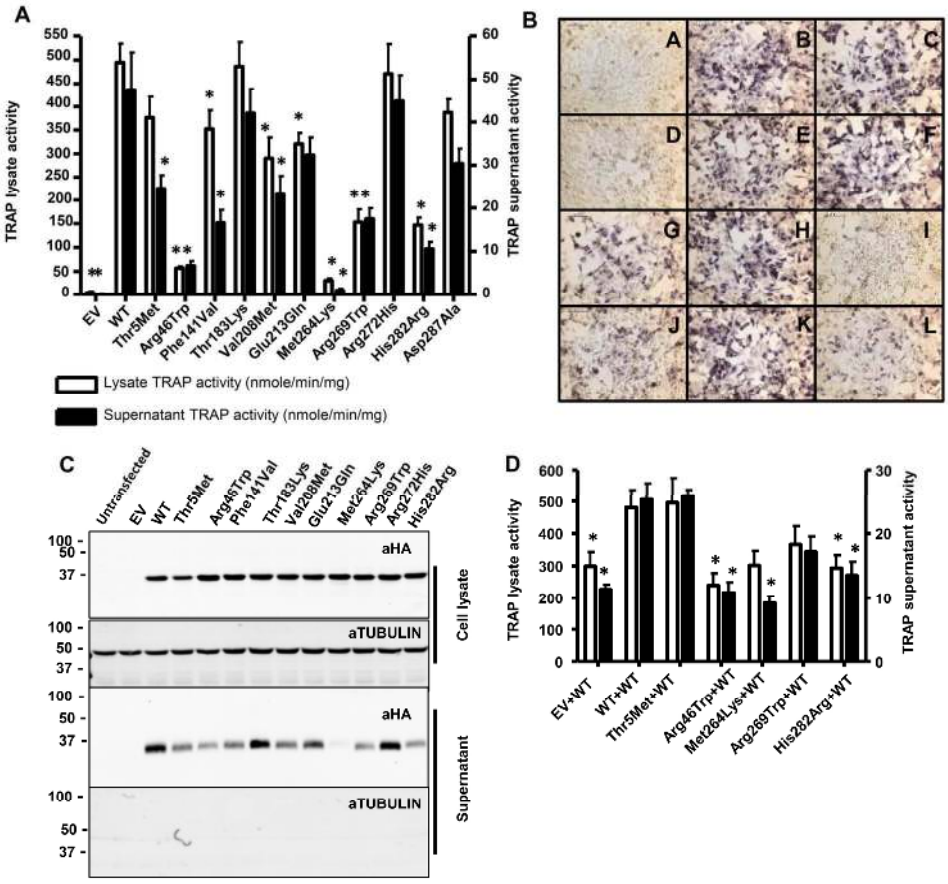

Figure6
173x158mm (300 x 300 DPI)

Supplementary Figures

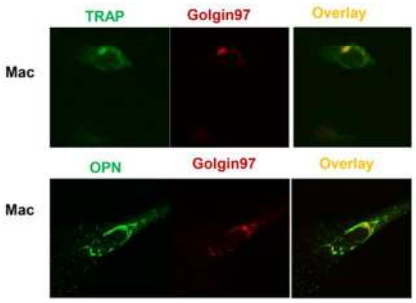

Supplementary Fig. 1. Localization of TRAP and OPN in primary macrophage cells. Confocal microscopy of Golgin97 (red) and TRAP (green, upper) or OPN (green, lower) in macrophage, demonstrate partial colocalization of both proteins in the Golgi. Representative image of four independent experiments.

100x53mm (300 x 300 DPI)

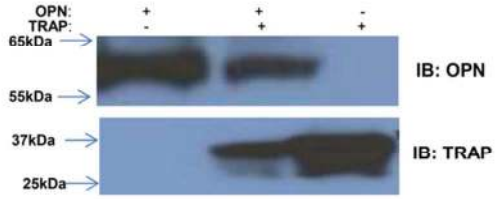

Supplementary Fig. 2. Overexpression of TRAP and OPN in HEK293 cells. Immunoblot (IB) of TRAP (upper panel) or OPN (lower panel) proteins following overexpression in HEK293 cells transfected with OPN, TRAP, or OPN and TRAP plasmids together as indicated in the legend above the figure. A representative image is shown from one of two independent experiments.

81x34mm (300 x 300 DPI)

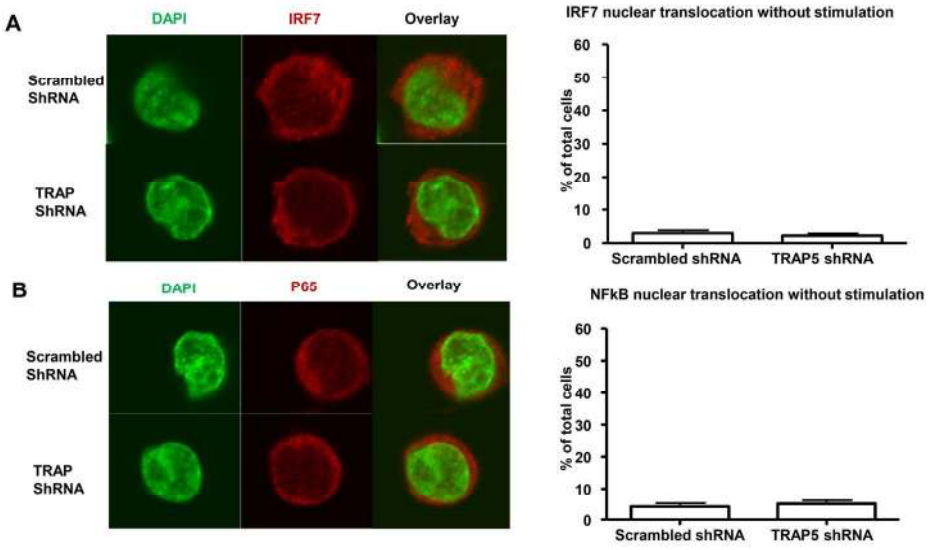

Supplementary Fig. 3. Localization of IRF7 and NFkB in unstimulated TRAP knockdown and scrambled pDCs.
The unstimulated pDC line, Gen 2.2, was analyzed by confocal microscopy using DAPI (pseudo-green) to stain the nucleus and an antibody to IRF7 (upper panel) or NFkB (lower panel) (pseudo-red). A representative image for both antibodies in TRAP KD pDCs compared to scrambled shRNA control was shown from two independent experiments. The % of cells with nuclear translocation without stimulation were quantified by ImageJ software and are shown in both cases in the graph on the right.

158x131mm (300 x 300 DPI)

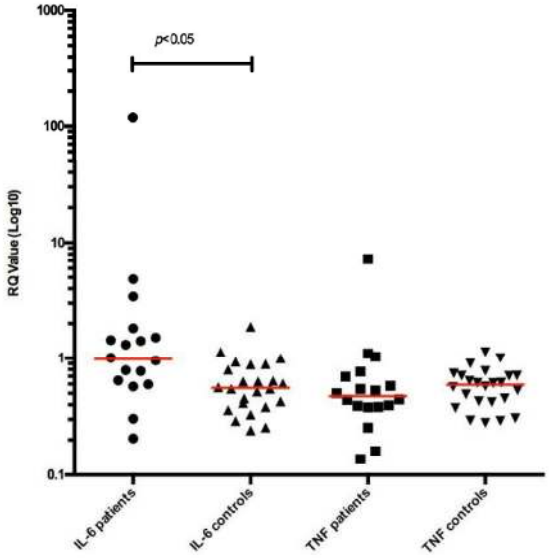

Supplementary Fig. 4. IL6 and TNF expression in SPENCD patients and controls. Quantitative reverse transcription PCR (qPCR) of IL-6 and TNFα expression in whole blood from 12 SPENCD patients (18 samples) compared to 24 healthy controls. Horizontal red bars show the median RQ value for each probe in each group. All values are shown for patients with biological replicates.

Blood was collected into PAXgene tubes and total RNA was extracted using a PAXgene RNA isolation kit (PreAnalytix). qPCR analysis was performed using the TaqMan Universal PCR Master Mix (Applied Biosystems) and cDNA derived from 40ng total RNA. The relative abundance of target transcripts, measured using TaqMan probes for IL6 (Hs00985639_m1) and TNFA (Hs99999043_m1), was normalized to the expression level of HPRT1 (Hs03929096_g1) and 18s (Hs999999001_s1) and assessed with the Applied Biosystems StepOne Software v2.1 and DataAssist Software v.3.01. For each probe, individual data were expressed relative to a single control calibrator. RQ is equal to 2-ΔΔCt i.e. the normalized fold change relative to a control. Each value is derived from four technical replicates. Data was analyzed by Kruskal-Wallis test using Dunn's multiple comparison test.

206x223mm (300 x 300 DPI)

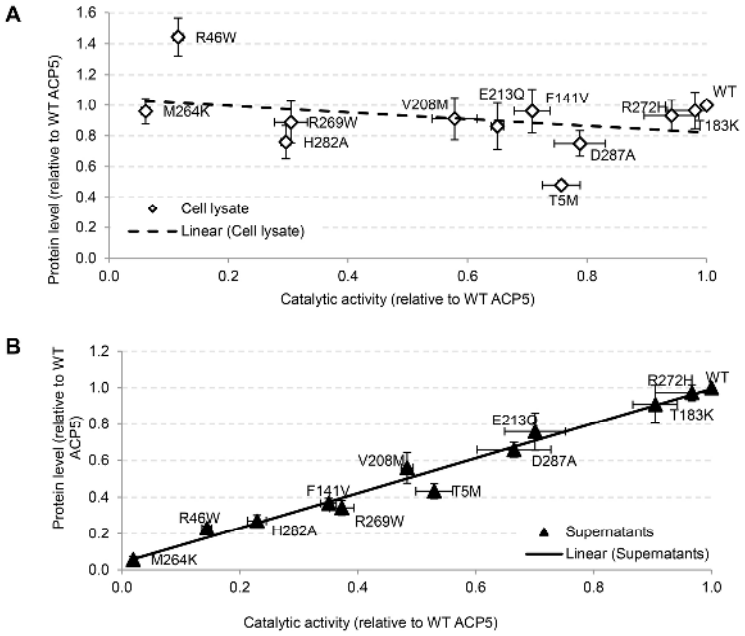

Supplementary Fig. 5: Pearson product moment correlation between activity and expression levels (relative to WT) in cell lysates and supernatants obtained from HEK293 cells transiently transfected with homozygous ACP5 variants identified in an SLE cohort.
Mean catalytic activity (n = 4-6, measured by PnPP assay) relative to WT TRAP is represented on the horizontal axis while mean relative expression level (n = 4, assessed by infrared western blot) is represented on the vertical axis for all ACP5 mutants analysed. The error bars represent the SEM. The line of best fit using Pearson's correlation is also displayed on the graph. A, The correlation between relative protein expression and activity in cell lysates was low (r2=0.107, r = -0.328, n=12). B, In the supernatant, a very high level of correlation (r2=0.977, r =0.989, n=12) was found between relative expression and activity.

183x177mm (300 x 300 DPI)

Supplementary Table 1: Rare missense heterozygote *ACP5* variants identified in the SLE and control cohorts.

Amino acid change	Allele count in SLE cohort	Pathogenic prediction using SIFT	Pathogenic prediction using Polyphen	Pathogenic prediction using Strater ([#] Strater, 2005)	In silico predicts pathogenic	Allele count in EXAC control database (MAF <0.002)*
Thr5Met	1/1950	Damaging (0)	Benign (0)	Not in crystal structure – not assessed	1/2	27/113638 (0.0002)
Arg27Ser	1/1950	Deleterious (0)	Probably damaging (0.968)	Deleterious (excess negative charge)	3/3	0
Arg46Trp	1/1950	Not damaging (0.19)	Probably damaging (0.998)	Deleterious (destabilisation or aggregation)	2/3	3/121082 (0.00002)
Val106Met^	1/1140	Deleterious (0.02)	Probably damaging (0.861)	Destabilisation	3/3	11/121410 (0.00009)
Gly109Arg^	1/1140	Deleterious (0.00)	Probably damaging (0.999)	Destabilisation	3/3	4/121410 (0.00003)
Phe141Val	1/1930	Not damaging (0.01)	Probably damaging (0.992)	Deleterious (likely to unfold protein)	2/3	17/121330 (0.0001)
Thr183Lys	1/1950	Not damaging (0.85)	Possibly damaging (0.39)	Not damaging	1/3	0
Val208Met	1/1950	Damaging (0.01)	Benign (0.195)	Deleterious (likely to unfold protein)	2/3	6/118174 (0.00005)
Glu213Gln	1/1950	Damaging (0.03)	Possibly damaging (0.66)	Deleterious (likely to unfold protein)	3/3	20/118060 (0.0002)
Met264Lys	1/1950	Not damaging (0.24)	Probably damaging (0.916)	Deleterious (charge burial uncompensated)	2/3	0
Arg269Trp	2/1950	Damaging (0.02)	Benign (0.015)	Deleterious (aggregation)	2/3	32/120358 (0.0003)
Arg272His	1/1950	Not damaging (0.17)	Possibly damaging (0.758)	Not damaging	1/3	25/120580 (0.0002)
His282Arg	1/1950	Not damaging (0.33)	Probably damaging (0.977)	Deleterious (likely to unfold protein)	2/3	0
Asp287Ala	2/1950	Not damaging (0.77)	Benign (0.012)	Not damaging	0/3	61/121168 (0.0005)
Pro320Leu	1/1950	Deleterious (0.01)	Benign (0.018)	Not damaging	1/3	3/120652 (0.000025)

241x306mm (300 x 300 DPI)

*None of these variants were seen in over 1000 alleles from in house matched controls.
^Variants observed in control cohort, whilst the remainder were in the SLE cohort.
#Strater N, Jasper B, Scholte M, Krebs B, Duff AP, Langley DB, et al. Crystal structures of recombinant human purple Acid phosphatase with and without an inhibitory conformation of the repression loop. J Mol Biol. 2005;351:233-46.

48x12mm (300 x 300 DPI)

Supplementary Table 2. Primers used for the qPCR quantification

18s	F	5' GAG GGA GCC TGA GAA ACG G 3'
	R	5' GTC GGG AGT GGG TAA TTT GC 3'
ACP5	F	5' CGG CCA CGA TCA CAA TCT 3'
	R	5' GCT TTG AGG GGT CCA TGA 3'
CXCL10	F	5' ATT TGC TGC CTT ATC TTT CTG 3'
	R	5' TCT CAC CCT TCT TTT TCA TTG TAG 3'
IFI27	F	5' CTC TAG GCC ACG GAA TTA ACC 3'
	R	5' CTC CTC CAA TCA CAA CTG TAG C 3'
IFI44L	F	5' GAA CTG GAC CCC ATG AAG G 3'
	R	5' ACT CTC ATT GCG GCA CAC C 3'
MX1	F	5' AGC CAC TGG ACT GAC GAC TT 3'
	R	5' ACC ACG GCT AAC GGA TAA G 3'
PKR	F	5' CTT CCA TCT GAC TCA GGT TT 3'
	R	5' TGC TTC TGA CGG TAT GTA TTA 3'

101x54mm (300 x 300 DPI)